Scientific Reports

Article in Press

Association of choroid plexus volume with brain atrophy and glucose metabolism in multiple system atrophy

Chae Jung Park, Yeeun Sun, Hyun-Jae Jeong, Han Kyu Na, So Hoon Yoon, Seung-Koo Lee, Chul Hyoung Lyoo, Young H. Sohn, Seong Ho Jeong & Phil Hyu Lee

We are providing an unedited version of this manuscript to give early access to its findings. Before final publication, the manuscript will undergo further editing. Please note there may be errors present which affect the content, and all legal disclaimers apply.

If this paper is publishing under a Transparent Peer Review model then Peer Review reports will publish with the final article.

Association of choroid plexus volume with brain atrophy and glucose metabolism in multiple system atrophy

Chae Jung Park, MD, PhD,[1*] Yeeun Sun, MD,[2*] Hyun-Jae Jeong,[3] Han Kyu Na, MD,[4] So Hoon Yoon, MD,[5] Seung-Koo Lee, MD, PhD,[6] Chul Hyoung Lyoo, MD, PhD,[7] Young H. Sohn, MD, PhD,[4] Seong Ho Jeong, MD,[4, 8, 9] Phil Hyu Lee, MD, PhD,[4]

[1] Department of Radiology, Yongin Severance Hospital, Yonsei University Health System, Yongin, South Korea

[2] Department of Neurology, Inje University Sanggye Paik Hospital, Seoul, South Korea

[3] Department of Pharmaceutics, Center for Pharmacometrics and Systems Pharmacology, College of Pharmacy, University of Florida, Orlando, Florida, USA

[4] Department of Neurology, Yonsei University College of Medicine, Seoul, South Korea

[5] Department of Neurology, National Health Insurance Service Ilsan Hospital, Goyang, South Korea

[6] Department of Radiology, Severance Hospital, Research Institute of Radiological Science and Centre for Clinical Imaging Data Science, Yonsei University College of Medicine, South Korea

[7] Department of Neurology, Gangnam Severance Hospital, Yonsei University College of Medicine, Seoul, South Korea

[8] Department of Neurology, Yongin Severance Hospital, Yonsei University Health System, Yongin, South Korea

[9] YONSEI BEYOND LAB, Yongin, South Korea

*These authors contributed equally to this work.

Address for correspondence:

Phil Hyu Lee, MD, PhD

Professor, Department of Neurology, Yonsei University College of Medicine

50 Yonsei-ro, Seodaemun-gu, Seoul, 03722, South Korea

Tel: 82-2-2228-1608; Fax: 82-2-393-0705

E-mail: phlee@yuhs.ac

Seong Ho Jeong, MD, PhD

Assistant Professor, Department of Neurology, Yongin Severance Hospital

363 Dongbaekjukjeon-daero, Giheung-gu, Yongin-si, Gyeonggi-do, 16995, South Korea

Tel: 82-31-5189-8146; Fax: 82-31-5189-8565

E-mail: seungho1987@yonsei.ac.kr

Running title: CP volume and MSA

Key words: multiple system atrophy; choroid plexus; brain atrophy; brain glucose metabolism

Abstract

The choroid plexus (CP), a component of the glymphatic system, is essential in homeostasis and producing cerebrospinal fluid. Roles of CP in multiple system atrophy (MSA) remains unclear. This study aimed to investigate the implication of the CP in MSA.

This retrospective cross-sectional study included 87 MSA patients who underwent the Unified MSA Rating Scale (UMSARS), brain MRI, and ^{18}F-fluorodeoxyglucose PET scan, along with 84 healthy controls (HCs). Multivariate linear regression analyses were performed to examine the associations between CP volume (CPV) and UMSARS scores, as well as the volumes and cerebral metabolism.

Compared with HCs, MSA had significantly reduced CPV (1.00 ± 0.27 vs. 1.30 ± 0.26, $P < 0.001$). CPV showed no association with UMSARS, however, it was positively correlated with regional cerebellar volumes. Reduced CPV was associated with lower cerebral glucose metabolism in MSA-susceptible regions, consistent with the positive association between CPV and regional cerebral glucose metabolism observed in multivariate analyses.. Notably, CPV positively correlated with glucose metabolism in the brainstem ($\beta = 0.110$, $P = 0.003$) and cerebellar white matter ($\beta = 0.080$, $P = 0.004$).

This study suggests that CPV is positively associated with disease burden in MSA, with CPV decreasing as disease severity increases. Further research is warranted to determine whether CPV could serve as a potential biomarker for MSA.

Key words: multiple system atrophy; choroid plexus; brain atrophy; brain glucose metabolism

Introduction

The choroid plexus (CP) is a highly vascularized structure located within the ventricles, composed of a network of capillaries lined by specialized epithelial cells. It is the principal source of cerebrospinal fluid (CSF) in the adult brain and plays a critical role in maintaining central nervous system homeostasis. Through the continuous secretion of CSF (approximately 400–600 mL per day), the CP contributes to regulating intracranial pressure, delivering nutrients and hormones to the brain, and facilitating the clearance of metabolic waste via the glymphatic system[1]. Notably, CP-driven CSF flow is crucial for the glymphatic pathway of waste removal, and disruptions in CSF production can impair the clearance of neurotoxic metabolites. Recent studies have demonstrated that an increase in CP volume (CPV) is closely associated with reduced glymphatic function[1-5].

An emerging body of evidence indicates that CPV is often increased in conditions associated with neurodegeneration, including Alzheimer's disease (AD), Parkinson's disease (PD), amyotrophic lateral sclerosis, and frontotemporal dementia[3,6-8]. Furthermore, our previous studies have demonstrated that enlarged CPV is associated with longitudinal outcome in patients with AD and PD[9,10]. These findings support the notion that the CP undergoes structural changes in response to neurodegenerative pathology, and that CP volumetry may serve as an indirect indicator of disease burden in certain disorders.

Multiple system atrophy (MSA) is a rare, rapidly progressive α-synucleinopathy characterized by a combination of parkinsonian features, cerebellar ataxia, autonomic failure, and pyramidal signs. As in other neurodegenerative diseases, reduced glymphatic function has been reported in MSA; however, research specifically addressing CPV and CP function in this condition remains limited[11]. Given its role in CSF dynamics, waste clearance, and immune cell trafficking, CPV assessment in MSA represents a novel approach to exploring disease pathophysiology. In this study, we examined CPV in patients with MSA compared to healthy controls (HCs), and we further evaluated the relationship between CPV, motor

4

symptoms, and imaging measures of disease severity—specifically, regional brain atrophy

and hypometabolism. We hypothesized that the CP is structurally affected in MSA and that

CPV correlates with the extent of neurodegeneration, thereby representing a potential

imaging biomarker of disease burden.

Result

Demographic and clinical characteristics of the study participants

This study included 87 patients with MSA and 84 healthy controls (HCs) (Figure 1). The

mean age at the time of magnetic resonance imaging (MRI) was significantly lower in the

MSA group compared with HCs, whereas sex distribution did not differ significantly between

the groups. Among patients with MSA, the mean disease duration from symptom onset to

MRI was 2.29 ± 1.46 years. The average UMSARS scores were 16.21 ± 8.51, 16.39 ± 8.29,

and 1.94 ± 1.09 for Parts I, II, and IV, respectively. The cerebellar subtype (MSA-C) was

more frequent than the parkinsonian subtype (MSA-P) (55.2% vs. 44.8%). The prevalence of

vascular risk factors, including hypertension, diabetes mellitus, and dyslipidemia, did not

differ significantly between the MSA and control groups (Table 1).

Imaging characteristics of the participants

Volumetric MRI revealed that CPV was significantly smaller in the MSA group compared

with controls. Hippocampal volume was also significantly reduced in patients with MSA.

Although lateral ventricle volume (LVV) tended to be larger in the MSA group, the difference

did not reach statistical significance. white matter hyperintensity volume (WMHV) was

significantly greater in patients with. Notably, total volumes of intracranium (ICV) was

markedly higher in the MSA group compared with controls (Table 1). When stratified by

MSA subtype, patients with both MSA-P and MSA-C exhibited significantly reduced CPV

5

and hippocampal volume compared with HCs, with no significant differences observed between the two subtypes. In these unadjusted group comparisons, no significant differences were observed in LVV or WMHV among the MSA-C, MSA-P, and control groups (Figure 2).

After adjusting for age at MRI scan and sex in multivariate linear regression model including MSA-P, MSA-C, and HCs, CPV remained significantly lower in both MSA-P (β = –0.240, P < 0.001) and MSA-C (β = –0.243, P < 0.001) compared with controls. Hippocampal volume was also significantly reduced in both subtypes, while LVV and WMHV were significantly higher, particularly in MSA-P. These findings indicate that volumetric alterations in MSA remain robust after controlling for demographic factors (Table 2). Thus, LVV and WMHV did not differ significantly between groups in unadjusted analyses (Table 1, Figure 2), but became evident in MSA, especially MSA-P, after adjusting for age and sex (Table 2). Similar results were observed in sensitivity analyses using absolute CPV with additional adjustment for ICV as a covariate, instead of normalization by the CPV/ICV ratio (Supplementary Table 1).

Partial correlation analyses within the MSA group, controlling for age at MRI scan, sex, and symptom duration, revealed a significant positive association between CPV and LVV (r = 0.600, P < 0.001). In contrast, CPV was not significantly associated with hippocampal volume (r = –0.204, P = 0.062) or WMHV (r = 0.100, P = 0.365). Given the significant association between CPV and LVV, subsequent analyses were adjusted for LVV as a covariate.

Relationship between CPV and regional brain atrophy

In the overall MSA cohort, CPV demonstrated significant positive correlations with both left and right cerebellar hemispheric structures, as well as midline vermian lobules, after adjusting for age, sex, symptom duration, and LVV. On the left side, CPV was positively

6

associated with cerebellar white matter, lobules I–IV, lobule V, lobule VI, and lobule VIIIb.

On the right side, significant associations were observed with cerebellar white matter, lobules

I–IV, lobule V, and lobule VIIIb. Additionally, CPV was positively correlated with midline

vermian structures, including vermis VI, VII, VIII, IX, and X. These associations remained

statistically significant after false discovery rate (FDR) correction for multiple comparisons.

In contrast, no significant associations were found between CPV and brainstem structures,

including the pons and medulla. In subgroup analyses, these positive correlations were

predominantly observed in patients with MSA-C, whereas associations in patients with MSA-

P were weaker and generally not statistically significant (Figure 3; Supplementary Table 2).

For other subcortical structures, multivariate linear regression analysis showed that

CPV was positively associated with bilateral ventral diencephalon volume in the overall MSA

group, and these associations remained significant after FDR correction. This relationship

was also observed in the MSA-C subgroup, whereas no significant associations were

observed in the MSA-P subgroup. No other subcortical structures, including the caudate,

putamen, pallidum, thalamus, or nucleus accumbens, demonstrated significant associations

with CPV after multiple comparisons (Supplementary Table 3).

Relationship between CPV and regional brain glucose metabolism

Multivariate linear regression analysis revealed that higher CPV was significantly associated

with increased regional glucose metabolism in several brain regions, after adjusting for age at

MRI, sex, symptom duration, and LVV (Supplementary Table 4). In the overall MSA cohort,

CPV showed significant positive associations with Cerebral Metabolic Rate for Glucose

(CMRglu) in the brainstem, cerebellar white matter, and bilateral thalamic and ventral

diencephalic regions, including the left thalamus, right thalamus, left ventral diencephalon,

7

and right ventral diencephalon. These associations remained significant after FDR correction for multiple comparisons.

In subgroup analyses, CPV was positively associated with CMRglu in the brainstem and cerebellar cortex in the MSA-P subgroup, and with the brainstem, cerebellar white matter, left thalamus, and right ventral diencephalon in the MSA-C subgroup. However, none of these associations in the subtype analyses remained significant after FDR correction. No significant associations were observed between CPV and CMRglu in basal ganglia structures, including the caudate, putamen, pallidum, and nucleus accumbens, in any group (Figure 4; Supplementary Table 4).

In the subset of 60 healthy controls with ^{18}F-fluorodeoxyglucose (FDG) PET data, nominal inverse associations were observed in the brainstem ($\beta = -0.089$, p = 0.025) and cerebellum ($\beta = -0.111$, p = 0.006), although these associations did not survive FDR correction (Supplementary Table 5), which indicates that the relationships identified in MSA are disease-specific rather than reflecting a general physiological coupling.

Relationship between CPV and motor symptoms

In multivariate linear regression analyses, CPV was not significantly associated with clinical severity, as measured by either individual or total the Unified MSA Rating Scale (UMSARS) scores, in the overall cohort or within MSA subtypes (Supplementary Table 6).

Discussion

In this study, we investigated the association between CPV, brain atrophy patterns, and cerebral metabolism in patients with MSA. The main findings were as follows: (1) CPV was reduced in patients with MSA compared to HCs. CPV in both the MSA-P and MSA-C subtypes was smaller than in HCs, although no inter-subtype differences were observed; (2)

8

CPV was positively associated with regional atrophy of subcortical structures, which are particularly vulnerable in MSA; and (3) CPV was positively associated with rCMRglu in MSA-related subcortical structures. Collectively, these findings suggest that CPV is decreased in patients with MSA and is positively associated with MSA-related neurodegeneration, indicating that CP atrophy may reflect disease severity in these patients.

We demonstrated that patients with MSA exhibit markedly reduced CPV compared with HCs. This finding stands in contrast to previous observations in other neurodegenerative diseases—notably PD and AD—where the CP has been reported to undergo volumetric enlargement [12]. The identification of CP atrophy in MSA is novel and suggests that the CP may respond differently to neuropathological processes in MSA than in PD or AD. To our knowledge, this is the first evidence that CPV is decreased in a neurodegenerative disorder, underscoring a disease-specific structural alteration that distinguishes MSA from the CP hypertrophy observed in AD, PD, and other neurodegenerative diseases[8,9,12-14].

The discrepant CPV changes observed between MSA and other neurodegenerative disorders likely reflect fundamental differences in underlying disease mechanisms and progression. In AD, CP enlargement and increased perfusion have been suggested as compensatory responses to protein accumulation[15]. whereas in MSA, CP atrophy may instead reflect exhaustion or degeneration. These findings have important implications for understanding the role of the CP in MSA. Similar to AD and PD, MSA is characterized by impaired protein clearance and has been linked to glymphatic system dysfunction[11]. The CP, as the primary source of CSF, is a critical component of the glymphatic clearance pathway, which facilitates the removal of metabolic waste products and aggregated proteins from the brain[16-18]. A reduction in CPV could therefore exacerbate glymphatic insufficiency in MSA by limiting CSF production and flow. Diminished CSF turnover may, in turn, hinder the clearance of toxic proteins and accelerate neurodegeneration. Conversely, chronic glymphatic

9

impairment in MSA—with consequent retention of neurotoxic proteins and inflammatory mediators—might contribute to structural damage and atrophy of the CP over time. Thus, a bidirectional relationship may exist whereby CP atrophy and glymphatic dysfunction reinforce one another, creating a vicious cycle of reduced waste clearance and progressive neural injury. From a temporal perspective, this raises the question of whether CP alterations in MSA may differ between early and later disease stages. Considering reports of increased CPV in other neurodegenerative disorders, it is plausible that CP changes may also occur in the early stage of MSA. However, given the rapidly progressive nature of MSA, such compensatory traits may be transient and subsequently diminish as the disease advances. In our cohort, the number of patients in the early stage (within 1 year of symptom onset) was limited (n=17), precluding a robust evaluation of early CP changes. Therefore, further studies with larger samples of very early-stage MSA, ideally using longitudinal designs, are warranted to clarify the temporal dynamics of CPV changes in MSA. Our observation of CPV reduction introduces a new perspective on MSA pathophysiology, supporting the concept that disruption of the cerebral fluid homeostatic systems—of which the CP is an integral component—contributes to neurodegenerative disease progression. While these interpretations remain speculative, they underscore a plausible link between CP structural integrity and the cerebral capacity to maintain homeostasis in the context of MSA's aggressive pathology.

In this study, CPV did not correlate with baseline clinical severity of motor symptoms in MSA. The lack of correlation with UMSARS may reflect the scale's limited sensitivity to CP-related processes[19]. In contrast, CPV in our MSA cohort showed significant positive correlations with neuroimaging biomarkers. Patients with larger CPV exhibited less regional brain atrophy on MRI—particularly in the cerebellar hemispheres and vermis—and higher regional glucose metabolism on FDG positron emission tomography (PET) in areas

vulnerable to MSA. In other words, a smaller CPV was associated with more severe

neurodegeneration across both structural and metabolic measures. Given that CPV was

reduced in patients with MSA compared with HCs, this pattern suggests that CPV may serve

as an indirect index of disease burden in MSA. The cerebellum and brainstem are among the

regions most affected in MSA, and it was within these areas that CPV correlations were most

pronounced. In MSA-C, where ataxia and cerebellar atrophy predominate, the associations

between CPV and preserved tissue volume were particularly robust. This may partly reflect

differences in regional atrophy patterns; while putaminal and caudate volumes were reduced

in MSA, their greater interindividual variability relative to cerebellar and brainstem structures

likely attenuated correlations with CPV[20]. In contrast, the more consistent and pronounced

posterior fossa atrophy in MSA-C may have facilitated clearer detection of associations

between CP and involved structures. A potential interpretation is that CP atrophy progresses

in parallel with cerebellar neurodegeneration, potentially due to shared pathogenic

mechanisms or localized interactions (e.g., the fourth ventricle CP directly interfaces with

cerebellar and brainstem structures). It is conceivable that a more intact CP confers

neuroprotective effects, potentially by sustaining adequate CSF production, growth factor

secretion, or immune surveillance, thereby mitigating tissue loss in connected regions[21].

Conversely, when CPV is reduced, these supportive functions may be compromised, leading

to greater accumulation of pathology and consequent atrophy and hypometabolism in MSA-

vulnerable regions. While causality cannot be established from our data, the clear association

between higher CPV and better-preserved brain structure and function reinforces the idea that

CP integrity is closely linked to overall brain health in MSA. Our cross-sectional baseline

analysis may have been underpowered to detect subtle clinical correlations, or the temporal

window during which CP changes align with motor symptom progression may be narrow.

11

Future longitudinal studies are needed to determine whether CPV has prognostic value for clinical progression, even if it does not reflect symptom severity at a single time point.

This study has some limitations and highlights future directions. First, our analysis was cross-sectional, which limits insight into the temporal dynamics of CP changes in MSA. We cannot determine whether CP atrophy represents a cause or a consequence of advanced neurodegeneration, or how early in the disease course it emerges. Longitudinal studies are needed to track CPV over time in MSA—for instance, to evaluate whether accelerated CPV loss parallels clinical deterioration or whether baseline CPV could stratify patients by prognosis. Second, although no consensus currently exists regarding the optimal reference region for FDG-PET in MSA, we selected the paracentral lobule based on prior findings indicating that its CMRglu is relatively spared in patients with MSA[22]. While the paracentral lobule has previously been used as a reference region in AD studies[23], this approach has not yet been applied in MSA. Since the choice of reference region can significantly influence the interpretation of regional glucose metabolism, particularly in disorders with widespread neurodegeneration, future work is needed to systematically evaluate and validate optimal normalization strategies for FDG-PET analysis in MSA. Third, given the rarity of MSA, our sample size—although relatively large for an MSA cohort—may still limit generalizability. Our cohort included both MSA-P and MSA-C subtypes across a range of disease durations; while we observed consistent CPV reductions across subtypes, subtle differences may have been overlooked. Replication of our findings in independent MSA cohorts, as well as direct comparisons with other synucleinopathies (e.g., comparing CPV in MSA vs. idiopathic PD directly), would further strengthen the evidence for a unique involvement of the CP in MSA. Fourth, genetic screening for RFC1 repeat expansions associated with CANVAS was not systematically performed, and therefore RFC1-related disorders cannot be completely excluded in this cohort[24]. However, all patients fulfilled established clinical criteria for MSA

12

and underwent comprehensive neurological evaluation with longitudinal follow-up., this remains a limitation and should be addressed in future studies incorporating systematic genetic testing.

In summary, we found that CPV was significantly decreased in patients with MSA compared with HCs, a contrasting pattern to that reported in PD and AD[3,17,25,26]. Furthermore, smaller CPVs in MSA were associated with greater brain atrophy and hypometabolism, suggesting that CP atrophy may serve as a marker of higher disease burden. Our findings highlight the CP as an essential and previously under-recognized contributor to MSA pathophysiology. Future studies integrating neuroimaging, biological, and clinical approaches are warranted to validate CPV as a potential imaging biomarker and to elucidate its mechanistic links to neurodegeneration in MSA.

Methods

Participants

We consecutively recruited 87 patients with MSA and 84 HCs from the Movement Disorders Outpatient Clinic of the Yonsei University Health System between 2008 and 2020. Patients with MSA were diagnosed with either clinically established MSA (n = 64) or clinically probable MSA (n = 23), according to the diagnostic criteria for MSA [27]. All patients underwent the Unified MSA Rating Scale (UMSARS; parts I–IV), brain MRI, and FDG-PET scan within 6 months. UMSARS was used to assess disease severity at the time of MRI acquisition. Total UMSARS score was defined as the sum of UMSARS-I (historical), UMSARS-II (motor examination), and UMSARS-IV (global disability scale) subscores. The diagnosis of MSA was further supported by structural and/or functional imaging findings, including atrophy on MRI of the putamen, middle cerebellar peduncle, pons, or cerebellum, as well as hypometabolism on FDG-PET in the putamen, brainstem, or cerebellum. None of

the patients carried mutations in the SCA 1, 2, 3, 6, 7, 8, and 17 genes.   All participants in

the HC group were recruited via poster advertisements for healthy older adults visiting

Severance Hospital. The HC group included 1) aged $\geq$ 50 years at enrollment, 2) the Korean

version of the Mini-Mental State Examination (K-MMSE) socre of $\geq$ 26, and 2) were able to

communicate in Korean, with written informed consent obtained after adequate

understanding of the study objectives and procedures. Individuals were excluded if they 1)

were unabile to adequately cooperate due to illiteracy, hearing impairment, or language

impairment, 2) had history of neurologic or psychiatric disorders, including infarction, severe

head trauma, brain surgery, major affective disorder, schizophrenia, or schizoaffective

disorder; (3) had contraindications to magnetic resonance imaging (MRI); or (4) participated

in other clinical studies involving radiation-based procedures during the study period. None

of the HCs reported cognitive impairment, and all demonstrated normal cognitive function

according to the K-MMSE and comprehensive neuropsychological testing. This study was

approved by the Institutional Review Board of Yonsei University Severance Hospital (IRB

No. 4-2024-1425 for patients with MSA; IRB No. 4-2015-0551 for HCs). All methods

involving participants were performed in accordance with relevant guidelines and

regulations, including the Declaration of Helsinki. The requirement for informed consent was

waived for patients with MSA due to the retrospective nature of the study; informed consent

for participation was obtained from all HCs.

MRI acquisition and analysis

All scans were acquired with a Philips 3.0T scanner (Philips Intera; Philips Medical System,

Best, The Netherlands) with a SENSE head coil (SENSE factor = 2). A high-resolution, T1-

weighted MRI volume data set was obtained from all subjects with a 3-dimensional T1-TFE

sequence configured with the following acquisition parameters: axial acquisition with a 224 ×

256 matrix; 256 × 256 reconstructed matrix with 182 slices; 220-mm field of view; 0.98 ×

0.98 × 1.2mm3 voxels; 4.6 ms echo time; 9.6 ms repetition time; 8° flip angle; and 0mm slice

gap. We used automated segmentation based on the same method as in our previous study, in

which the accuracy of this approach was validated. [12] Automated segmentation of brain

regions and the cortical thickness values of each region were extracted using FastSurfer,

which is a fast and extensively validated deep-learning pipeline for the fully automated

processing of structural human brain MRIs[27]. This software enabled whole-brain

segmentation into 95 classes within 50 seconds per subject. The details of this program and

its validity have been shown elsewhere (https://deep-mi.org/research/fastsurfer/). A

representative automatic segmentation of the CP using FastSurfer is shown in Supplementary

Figure 1. In a subset of 30 patients, we manually segmented the CPV to assess inter-method

reliability. One neuroradiologist (C.J.P., with six years of experience) manually segmented

the CP in the lateral ventricle in the 3D T1-weighted volumetric images using 3D Slicer

version 5.0.3 (https://www.slicer.org). From these images, the ICV, LVV, WMHV,

hippocampus, amygdala, basal ganglia, thalamus, ventral diencephalon, pons, and medulla

were obtained. Further, detailed sub-segmentation of cerebellum was performed to achieve

volumetric results of crus, lobules, vermis, and white matter. All final automatic segmentation

results were checked and approved by a single neuroradiologist (C.J.P.) without subsequent

manual correction. The regional volumes were expressed as the ratio of the regional volume

to the total ICV (ratio of ICV × 10^3).

Acquisition and quantitative analyses of ^{18}F-FDG PET

FDG-PET scans were performed using a Discovery 600 scanner (General Electric Healthcare,

Milwaukee, MI, USA). FDG-PET scans were performed according to the following protocol:

Approximately 4.1 MBq/kg (body weight) ^{18}F-FDG was administered intravenously to the

patient. After a 60-minute uptake period, PET images were acquired for 15 minutes. A spiral

computed tomography scan was performed for attenuation correction with a 0.8 second

rotation time at 60 mA and 120 kVp, and with 3.75 mm section thickness, 0.625 mm

collimation, and 9.375 mm table feed per rotation. FDG-PET images were reconstructed

using the ordered subset expectation maximization algorithm with 4 iterations and 32 subsets.

To assess brain glucose metabolism in each participant using FDG-PET imaging, Statistical

Parametric Mapping 12 (SPM12; Wellcome Trust Centre for Neuroimaging, London, UK)

and in-house software implemented in MATLAB R2021a (MathWorks, Natick, MA) were

used. Structural MRI images were segmented and spatially normalized to the Montreal

Neurological Institute (MNI) space for each participant. The FDG-PET images were co-

registered to the corresponding T1-weighted images. The Standard uptake value ratio

(SUVR) of FDG-PET was calculated by overlaying a participant-specific composite volume

of interest (VOI) onto the FDG PET images. The SUVR images were generated using the

uptake value of paracentral lobule as the reference. The paracentral lobule was chosen as the

reference region based on comparative analyses with 60 HCs who underwent FDG PET

imaging among the total cohort of 84 HCs, in which it was the only region showing no

statistically significant difference in raw FDG uptake, unlike other cortical and subcortical

areas that demonstrated marked differences (Supplementary Table 7). The preprocessed

SUVR images were smoothed using a 6mm full-width at half maximum (FWHM) Gaussian

kernel.

Statistical analysis

The baseline clinical and imaging characteristics of the study participants were analyzed

using independent t-tests or one-way ANOVA for continuous variables when normality was

confirmed by the Shapiro-Wilk test; otherwise, non-parametric tests such as the Mann–

Whitney U test or Kruskal–Wallis test were applied. Categorical variables were analyzed

using the chi-square or Fisher's exact tests, as appropriate. Normality of distribution was

assessed using Shapiro-Wilk test. Partial correlation analyses, adjusted for age and sex, were

conducted within the MSA group to examine the relationships between CPV and other

imaging parameters including LVV, hippocampal volume, and WMHV.

　　　To identify the independent effect of CPV on motor symptoms assessed using

UMSARS total scores at initial visit, multivariate linear regression analysis was performed

after adjusting for age at symptom onset, sex, symptom duration, and LVV. Multivariate

linear regression analyses for regional brain atrophy and CMRglu were performed to explore

the effect of CPV on MSA-related neurodegeneration after adjusting for age at symptom

onset, sex, symptom duration, and LVV. The FDR method was used to correct multiple tests.

Statistical analyses were performed using the R software (v4.0, http://www.r-project.org).

Results with a two-tailed *P* value < 0.05 were considered statistically significant.

Reference

1　　　Kratzer, I., Ek, J. & Stolp, H. The molecular anatomy and functions of the choroid
　　　plexus in healthy and diseased brain. *Biochim Biophys Acta Biomembr* **1862**, 183430
　　　(2020). https://doi.org/10.1016/j.bbamem.2020.183430

2　　　Mogensen, F. L., Delle, C. & Nedergaard, M. The Glymphatic System (En)during
　　　Inflammation. *Int J Mol Sci* **22** (2021). https://doi.org/10.3390/ijms22147491

3　　　Harrison, I. F. *et al.* Impaired glymphatic function and clearance of tau in an
　　　Alzheimer's disease model. *Brain* **143**, 2576-2593 (2020).
　　　https://doi.org/10.1093/brain/awaa179

4　　　Ricigliano, V. A. G. *et al.* Choroid Plexus Enlargement in Inflammatory Multiple
　　　Sclerosis: 3.0-T MRI and Translocator Protein PET Evaluation. *Radiology* **301**, 166-
　　　177 (2021). https://doi.org/10.1148/radiol.2021204426

5　　　Liu, R. *et al.* Choroid plexus epithelium and its role in neurological diseases. *Front
　　　Mol Neurosci* **15**, 949231 (2022). https://doi.org/10.3389/fnmol.2022.949231

6   Tadayon, E., Pascual-Leone, A., Press, D. & Santarnecchi, E. Choroid plexus volume is associated with levels of CSF proteins: relevance for Alzheimer's and Parkinson's disease. *Neurobiol Aging* **89**, 108-117 (2020). https://doi.org/10.1016/j.neurobiolaging.2020.01.005

7   Tadayon, E. *et al.* Improving Choroid Plexus Segmentation in the Healthy and Diseased Brain: Relevance for Tau-PET Imaging in Dementia. *J Alzheimers Dis* **74**, 1057-1068 (2020). https://doi.org/10.3233/jad-190706

8   Dai, T. *et al.* Choroid plexus enlargement in amyotrophic lateral sclerosis patients and its correlation with clinical disability and blood-CSF barrier permeability. *Fluids Barriers CNS* **21**, 36 (2024). https://doi.org/10.1186/s12987-024-00536-6

9   Liu, L. *et al.* Choroid plexus enlargement contributes to motor severity via regional glymphatic dysfunction in Parkinson's disease. *NPJ Parkinsons Dis* **11**, 134 (2025). https://doi.org/10.1038/s41531-025-00971-8

10   Jeong, S. H. *et al.* Association between choroid plexus volume and cognition in Parkinson disease. *Eur J Neurol* **30**, 3114-3123 (2023). https://doi.org/10.1111/ene.15999

11   Shi, C. *et al.* Impaired glymphatic clearance in multiple system atrophy: A diffusion spectrum imaging study. *Parkinsonism Relat Disord* **123**, 106950 (2024). https://doi.org/10.1016/j.parkreldis.2024.106950

12   Jeong, S. H. *et al.* Choroid Plexus Volume, Amyloid Burden, and Cognition in the Alzheimer's Disease Continuum. *Aging Dis* **16**, 552-564 (2024). https://doi.org/10.14336/ad.2024.0118

13   Assogna, M. *et al.* Association of Choroid Plexus Volume With Serum Biomarkers, Clinical Features, and Disease Severity in Patients With Frontotemporal Lobar Degeneration Spectrum. *Neurology* **101**, e1218-e1230 (2023). https://doi.org/10.1212/wnl.0000000000207600

14   Wang, N. *et al.* Choroid plexus enlargement correlates with subcortical tau deposition in progressive supranuclear palsy. *Fluids Barriers CNS* **22**, 52 (2025). https://doi.org/10.1186/s12987-025-00663-8

15   Li, J. *et al.* Associations between the choroid plexus and tau in Alzheimer's disease using an active learning segmentation pipeline. *Fluids Barriers CNS* **21**, 56 (2024). https://doi.org/10.1186/s12987-024-00554-4

16   Shi, C. *et al.* Impaired glymphatic clearance in multiple system atrophy: A diffusion

spectrum imaging study. *Parkinsonism & Related Disorders* **123**, 106950 (2024). https://doi.org/https://doi.org/10.1016/j.parkreldis.2024.106950

17   Municio, C., Carrero, L., Antequera, D. & Carro, E. Choroid Plexus Aquaporins in CSF Homeostasis and the Glymphatic System: Their Relevance for Alzheimer's Disease. *Int J Mol Sci* **24** (2023). https://doi.org/10.3390/ijms24010878

18   Braun, M. & Iliff, J. J. The impact of neurovascular, blood-brain barrier, and glymphatic dysfunction in neurodegenerative and metabolic diseases. *Int Rev Neurobiol* **154**, 413-436 (2020). https://doi.org/10.1016/bs.irn.2020.02.006

19   Jessen, N. A., Munk, A. S., Lundgaard, I. & Nedergaard, M. The Glymphatic System: A Beginner's Guide. *Neurochem Res* **40**, 2583-2599 (2015). https://doi.org/10.1007/s11064-015-1581-6

20   Palma, J. A. *et al.* Limitations of the Unified Multiple System Atrophy Rating Scale as outcome measure for clinical trials and a roadmap for improvement. *Clin Auton Res* **31**, 157-164 (2021). https://doi.org/10.1007/s10286-021-00782-w

21   Chelban, V. *et al.* An update on advances in magnetic resonance imaging of multiple system atrophy. *J Neurol* **266**, 1036-1045 (2019). https://doi.org/10.1007/s00415-018-9121-3

22   Tsitsou-Kampeli, A., Suzzi, S. & Schwartz, M. The immune and metabolic milieu of the choroid plexus as a potential target in brain protection. *Trends Neurosci* **47**, 573-582 (2024). https://doi.org/10.1016/j.tins.2024.05.010

23   Park, K. W. *et al.* Cortical hypometabolism associated with cognitive impairment of multiple system atrophy. *Parkinsonism Relat Disord* **81**, 151-156 (2020). https://doi.org/10.1016/j.parkreldis.2020.10.039

24   Jiang, J. *et al.* Study of the Influence of Age in (18)F-FDG PET Images Using a Data-Driven Approach and Its Evaluation in Alzheimer's Disease. *Contrast Media Mol Imaging* **2018**, 3786083 (2018). https://doi.org/10.1155/2018/3786083

25   Ding, X. B. *et al.* Impaired meningeal lymphatic drainage in patients with idiopathic Parkinson's disease. *Nat Med* **27**, 411-418 (2021). https://doi.org/10.1038/s41591-020-01198-1

26   Serot, J. M., Béné, M. C., Foliguet, B. & Faure, G. C. Morphological alterations of the choroid plexus in late-onset Alzheimer's disease. *Acta Neuropathol* **99**, 105-108 (2000). https://doi.org/10.1007/pl00007412

27   Wenning, G. K. *et al.* The Movement Disorder Society Criteria for the Diagnosis of

Multiple System Atrophy. *Mov Disord* **37**, 1131-1148 (2022). https://doi.org/10.1002/mds.29005

28   Henschel, L. *et al.* FastSurfer - A fast and accurate deep learning based neuroimaging pipeline. *Neuroimage* **219**, 117012 (2020). https://doi.org/10.1016/j.neuroimage.2020.117012

Acknowledgements

Funding

Author contributions

C.J.P., Y.S., S.H.J., and P.H.L. conceptualized and designed the study. Y.S., H.K.N., S.K.L., Y.H.S., and P.H.L contributed to the acquisition of the data. C.J.P., Y.S., H.J.J., C.H.L., and S.H.J. contribute to analysis of the data. C.J.P., Y.S., S.H.J., and P.H.L. drafted and/or revised the manuscript. S.H.J., and P.H.L. is the gaudrantor.

Data availability statement

Data generated or analyzed during the study are available from the corresponding author by request.
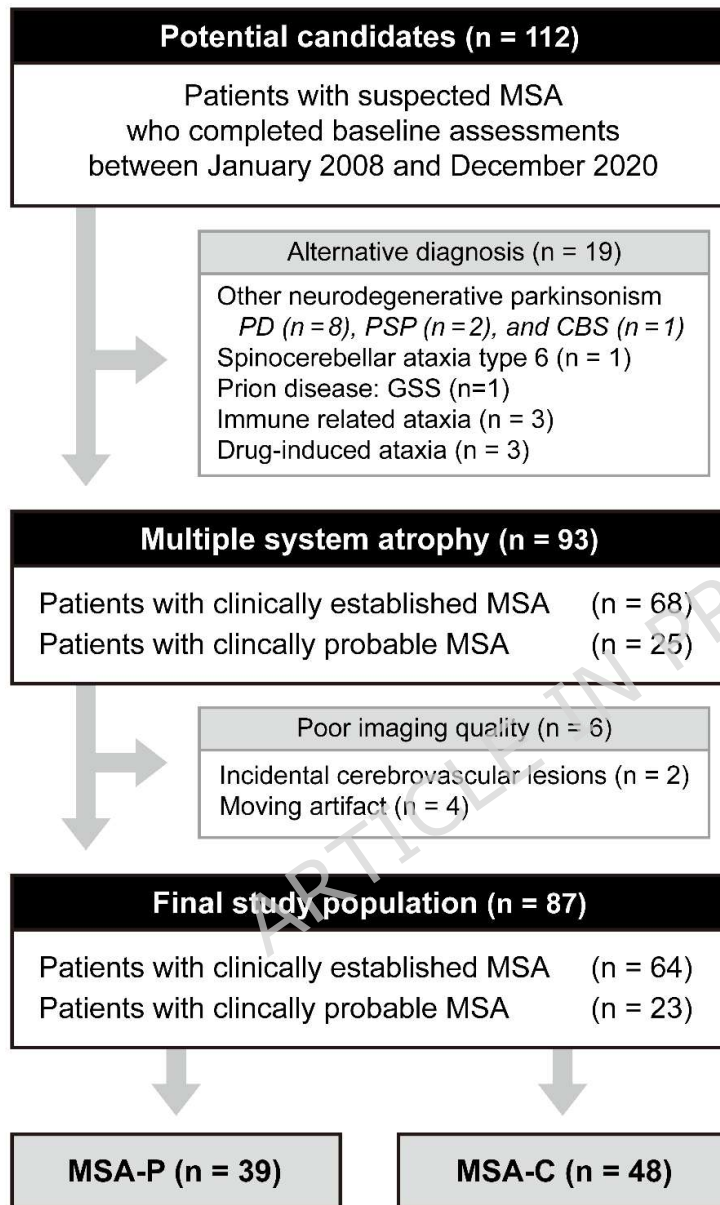
Competeing interests

The authors declare no conflicts of interest. There are no financial disclosures.

Supplementary Information

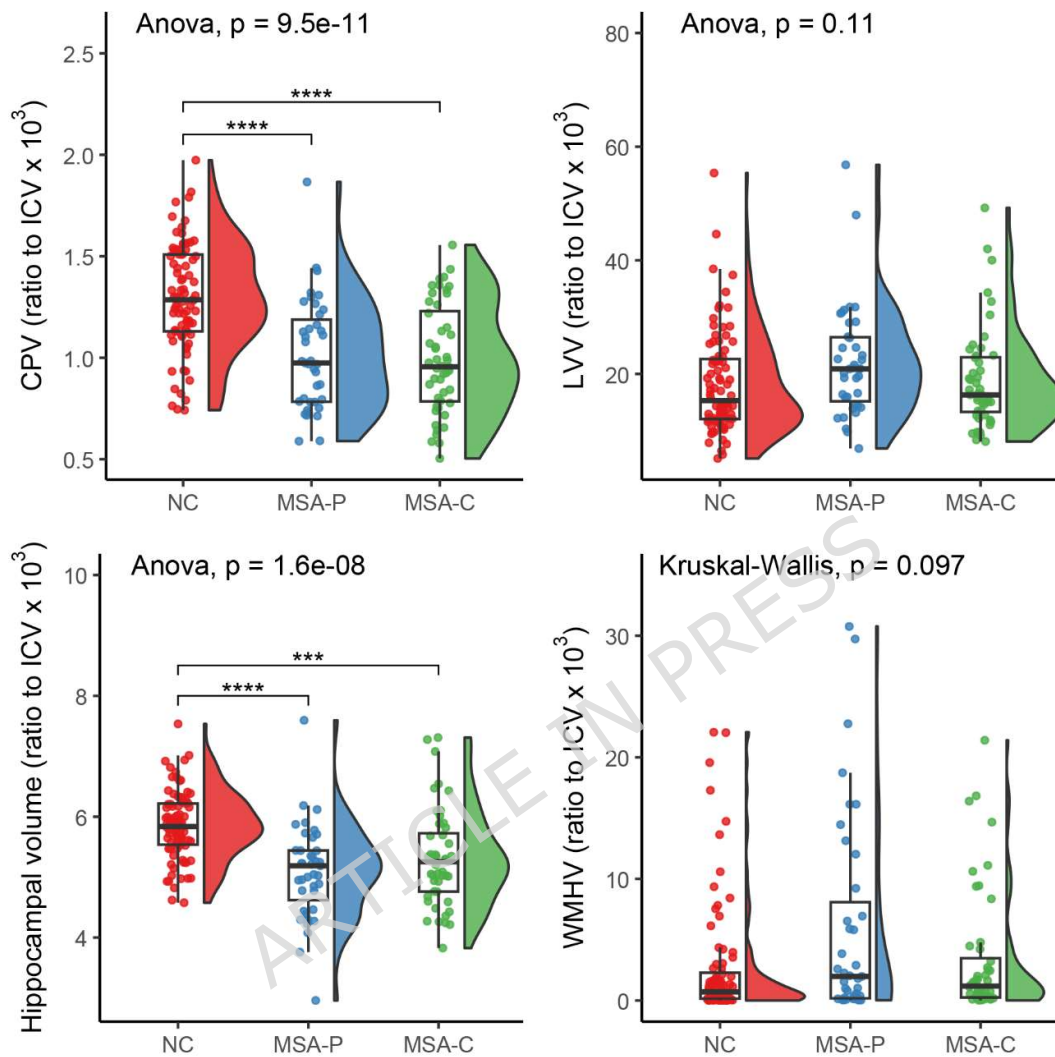The online version contains supplementary material available

Figure legends

Figure 1. Flow diagram of the study sample

CBS = Corticobasal syndrome, GSS = Gerstmann–Sträussler–Scheinker syndrome, MSA = Multiple system atrophy, MSA-P = Multiple system atrophy-parkinsonian type, MSA-C = Multiple system atrophy-cerebellar type, PD = Parkin disease, PSP = Progressive supranuclear palsy.
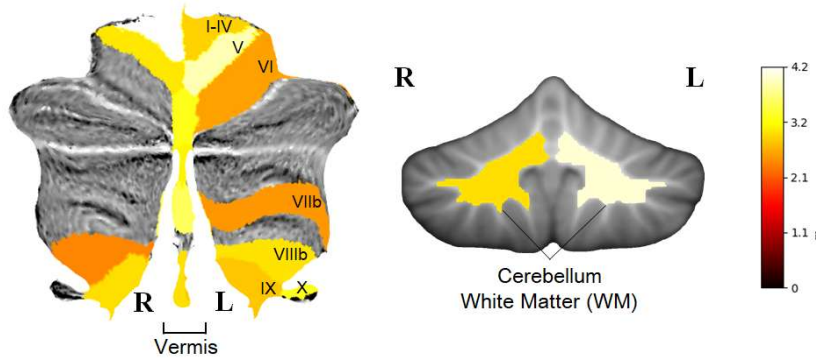
Figure 2. Rain-cloud plots of MR volumetric imaging markers, including CPV, LVV, hippocampal volume, and WMHV in the HC, MSA-P, and MSA-C groups.
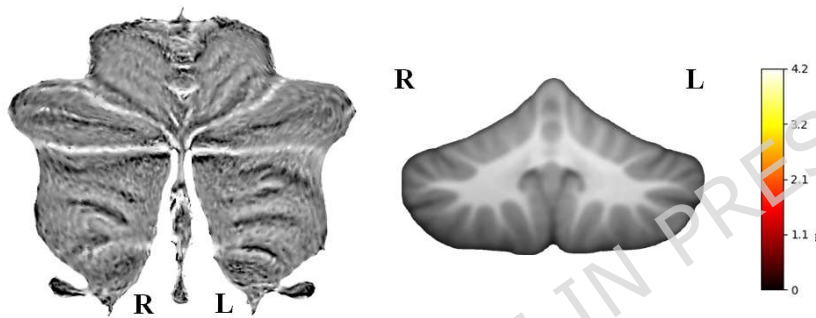

MR = magnetic resonance; CPV = choroid plexus volume; LVV = lateral ventricle volume; WMHV = white matter hyperintensity volume; MSA-P = multiple system atrophy-parkinsonian type; multiple system atrophy-cerebellar type; *** uncorrected $P < 0.001$;

**** uncorrected $P < 0.0001$.

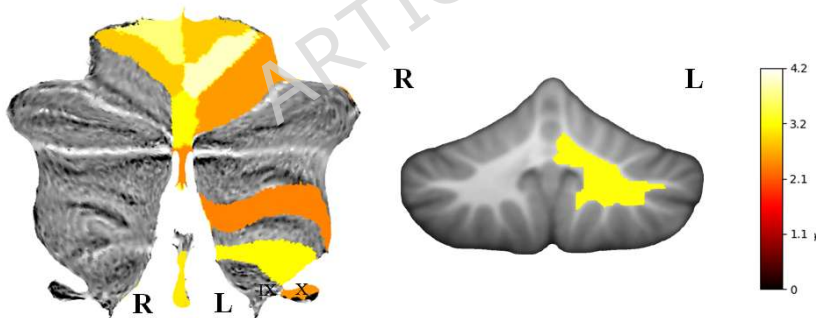**Figure 3. Relationship between CPV and cerebellar brain volumes.**

(A) Whole patients with MSA (n = 87)

(B) Patients with MSA-P (n = 39)

(C) Patients with MSA-C (n = 48)

Regions showing a significant association between CPV and regional cerebellar volume are visualized on a cerebellar heatmap template, with color indicating t-values derived from a multivariate linear regression model in (A) all patients with MSA, (B) patients with MSA-P, and (C) patients with MSA-C. CPV = choroid plexus volume; MSA = multiple system atrophy; MSA-P = multiple system atrophy-parkinsonian type; multiple system atrophy-cerebellar type.

24

Figure 4. Relationship between CPV and subcortical cerebral glucose metabolism.

Regions showing a significant association between CPV and subcortical cerebral glucose metabolism are visualized on the aseg subcortical atlas, with color indicating t-values derived from a multivariate linear regression model in patients with MSA. CPV = choroid plexus volume; MSA = multiple system atrophy.

Table 1. Demographic and imaging characteristics in patients with MSA and healthy controls

	Patients with MSA (n = 87)	Healthy controls (n = 84)	P
Demographic characteristics			
Age at symptom onset, y	60.60 ± 8.80	-	NA
Age at MRI scan	62.88 ± 8.89	66.48 ± 9.40	0.011
Female	44 (50.6%)	46 (54.8%)	0.693
Symptom duration (onset to MRI scan), y	2.29 ± 1.46	-	NA
UMSARS			
Part I	16.21 ± 8.51	-	NA
Part II	16.39 ± 8.29	-	NA
Part IV	1.94 ± 1.09	-	NA
Subtype			
Parkinsonian type	39 (44.8%)	-	NA
Cerebellar type	48 (55.2%)	-	NA
Vascular risk factors			
Hypertension	56 (35.6%)	23 (27.4%)	0.319
Diabetes mellitus	17 (19.5%)	8 (9.5%)	0.102
Dyslipidemia	25 (28.7%)	21 (25.0%)	0.705
Volumetric MRI measures			
CP volume, ratio of ICV $\times 10^3$	1.00 ± 0.27	1.30 ± 0.26	<0.001
hippocampal volume, ratio of ICV $\times 10^3$	5.21 ± 0.80	5.86 ± 0.57	<0.001
LV volume, ratio of ICV $\times 10^3$	20.38 ± 9.40	18.32 ± 9.06	0.147
WMH volume, ratio of ICV $\times 10^3$	4.57 ± 6.87	2.76 ± 4.95	0.049
ICV, mL	1512.68 ± 197.84	1365.40 ± 135.42	<0.001

Values are expressed as mean ± standard deviation or number (percentage).

CP = choroid plexus; ICV = intracranial volume; LV = lateral ventricle; MRI = magnetic resonance imaging; MSA = multiple system atrophy; NA = not applicable/available; UMSARS = Unified Multiple System Atrophy Rating Scale; WMH = white matter hyperintensity.

Table 2. Multivariate linear regression analysis for CPV in relation to brain volume measures

	CPV				LVV				Hippocampal volume				WMHV			
	B	*SE*	*t*	*P*	*β*	*SE*	*t*	*P*	*β*	*SE*	*t*	*P*	*β*	*SE*	*t*	*P*
Intercept	0.366	0.134	2.735	0.007	-17.927	4.598	-3.899	<0.001	7.887	0.339	23.27	<0.001	-20.29	3.005	-6.752	<0.001
Age	0.016	0.002	8.875	<0.001	0.590	0.063	9.356	<0.001	-0.041	0.005	-8.735	<0.001	0.374	0.041	9.090	<0.001
Sex	-0.096	*0.034*	-2.871	0.005	-1.902	1.155	-1.646	0.102	0.433	0.085	5.088	<0.001	-1.185	0.755	-1.569	0.119
Group																
HC	Ref.				Ref.				Ref.				Ref.			
MSA-P	-0.240	0.042	-5.680	<0.001	5.247	1.455	3.606	<0.001	-0.899	0.107	-8.384	<0.001	4.156	0.951	4.370	<0.001
MSA-C	-0.243	0.040	-6.007	<0.001	3.165	1.388	2.280	0.024	-0.680	0.102	-6.648	<0.001	2.258	0.907	2.489	0.014

Results of multivariate linear regression analysis for the CPV, LVV, hippocampal volume, or WMHV after controlling for age at MRI scan, sex, and group. CPV = choroid plexus volume; LVV = lateral ventricle volume; MRI = magnetic resonance imaging; HC = healthy control; MSA-P = multiple system atrophy-parkinsonian type; multiple system atrophy-cerebellar type; WMHV = white matter hyperintensity volume.